Proceedings of the 9th International Symposium on
Dynamics and Control of Process Systems (DYCOPS 2010),
Leuven, Belgium, July 5-7, 2010
Mayuresh Kothare, Moses Tade, Alain Vande Wouwer, Ilse Smets (Eds.)

Lattice-size Dependence and Dynamics of Surface Mean Slope in a Thin Film Deposition Process ⋆

Jianqiao Huang * **Gangshi Hu** * **Gerassimos Orkoulas** *
Panagiotis D. Christofides *,**

* *Department of Chemical and Biomolecular Engineering*
University of California, Los Angeles, CA 90095-1592
** *Department of Electrical Engineering*
University of California, Los Angeles, CA 90095-1592

Abstract: This work focuses on the study of the dynamic behavior and lattice size dependence of the surface root-mean-square slope in a porous thin film deposition process taking place on a triangular lattice. The simulation results indicate that the expected mean slope square reaches quickly a steady-state value and exhibits a very weak dependence with respect to lattice size variation. The simulation findings are corroborated by an analysis of appropriate finite-difference discretizations of surface height profiles computed by an Edwards-Wilkinson-type partial differential equation that can be used to describe the dynamics of surface height profile in the thin film deposition process under consideration.

Keywords: Root-mean-square slope, stochastic PDEs, thin film deposition process, kinetic Monte-Carlo simulations.

1. INTRODUCTION

Photovoltaic cells (solar cells) constitute an important source of sustainable energy. However, the limited conversion efficiency of the solar power prevents the wide application of solar cells, including thin-film silicon solar cells. Research on optical and electrical modeling of thin-film silicon solar cells indicates that the scattering properties (light reflectance and transmittance) of the thin film interfaces are directly related to the light trapping processes and the efficiency of thin-film silicon solar cells (e.g., Krč et al. (2003); Müller et al. (2004)). For example, a higher diffused transmittance of incident light is desired for the upper surface of solar cells for a maximum energy input into the semiconductor layers. The scattering properties of the interfaces depend strongly on the film surface morphology, which includes root-mean-square (RMS) roughness and RMS slope (Vorburger et al. (1993)). Thus, for the purposes of improving the conversion efficiency of thin-film solar cells, desired film surface RMS roughness and slope levels should be attained during the manufacturing process.

Kinetic Monte Carlo (kMC) methods have been widely used to simulate thin film microscopic process by utilizing microscopic film growth processes and kinetics that are obtained from molecular dynamic simulations and experiments (Levine et al. (1998); Zhang et al. (2004); Levine and Clancy (2000); Lou and Christofides (2003); Christofides et al. (2008)). However, the high computational cost that kMC simulations require prevents their use for real-time monitoring and control purposes. Alternatively, stochastic differential equation (SDE) models can be used in the modeling of surface morphology of thin films to describe the evolution of surface height profiles and surface roughness in a variety of thin film preparation processes (Edwards and Wilkinson (1982); Kardar (2000)). Recently, modeling and control of thin film microstructure using SDE models has attracted significant attention (Ni and Christofides (2005); Christofides et al. (2008); Hu et al. (2009b,d,c)). However, the dynamics and control of RMS slope of surface height profiles in thin film deposition processes has not been studied.

This work focuses on the study of the dynamic behavior and lattice size dependence of the surface root-mean-square slope in a porous thin film deposition process taking place on a triangular lattice. The thin film deposition process involves atom adsorption and migration and is described by a kMC simulation. The simulation results indicate that the expected mean slope square reaches quickly a steady-state value and exhibits a very weak dependence with respect to lattice size variation. The simulation findings are corroborated by an analysis of appropriate finite-difference discretizations of surface height profiles computed by an Edwards-Wilkinson (EW)-type partial differential equation (PDE) that can be used to describe the dynamics of surface height profile in the thin film deposition process under consideration.

2. POROUS THIN FILM DEPOSITION PROCESS

In this section, a porous thin film deposition process is considered and modeled by using an on-lattice kMC model on a triangular lattice in which vacancies and overhangs are allowed to develop (Hu et al. (2009d,a)). In this deposition process, the film surface morphology is

⋆ Financial support from NSF, CBET-0652131, is gratefully acknowledged. Panagiotis D. Christofides is the corresponding author (e-mail: pdc@seas.ucla.edu).

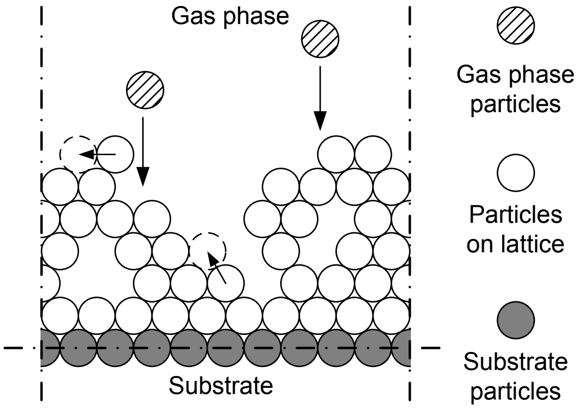

Fig. 1. Thin film growth process on a triangular lattice. The arrows denote adsorption and migration processes.

determined by two micro-processes: an adsorption process and a migration process. The definitions of surface height profile and root-mean-square slope are also introduced.

2.1 On-lattice kinetic Monte Carlo model

Fig. 1 shows the thin film growth process taking place on a two-dimensional triangular lattice. In this lattice model, lattice size denotes the number of sites in the lateral direction per layer, i.e., the maximum number of particles that can be packed within one horizontal layer. The coordination number of the triangular lattice is six, so a particle on the lattice can have at most six nearest neighbors. Periodic boundary conditions (PBCs) are applied to the lattice model. In the bottom of the lattice, a fully-packed and fixed substrate layer is initially placed to initiate the thin film deposition process.

We consider two different types of micro-processes in the deposition process: an adsorption process and a migration process. In an adsorption process, incident particles are deposited from the gas phase and are incorporated into the thin film. In this work, only vertical incidence is considered in the adsorption process. When an incident particle is incorporated into the film, it moves to the nearest vacant site of the contacting particle. If the incident particle moves to a site that has only one nearest neighbor, this particle is unstable in the two-dimensional lattice. An unstable particle is subject to instantaneous relaxation process, where it moves to the most stable vacant site neighboring the unstable site, i.e., the site that has the most nearest neighbors.

In a migration process, particles on the thin film overcome the energy barrier of their sites and move to their adjacent vacant sites (Wang and Clancy (2001); Yang et al. (1997)). Substrate particles cannot move. The migration rate follows an Arrhenius-type law, where the pre-exponential factor and the activation energy are taken from a silicon film (see Hu et al. (2009a) for details). We note that the migration process is executed for stable particles on the lattice that have vacant neighboring sites, which makes the migration process different from the instantaneous relaxation process occurring during an adsorption event.

The microscopic rules of the micro-processes are used in a kMC method to simulate the thin film deposition process. Specifically, a continuous-time Monte Carlo (CTMC)-type method (e.g., Vlachos et al. (1993)) is used to carry out the kMC simulations. KMC simulations generate realizations of the microscopic thin film deposition process. The thin film microstructure is obtained during the kMC simulations and is the result of a complex interplay between adsorption and migration processes. The two macroscopic operating variables of the deposition process that influence the resulting film microstructure are the adsorption rate and the substrate temperature. The adsorption rate, which is denoted by W, is defined as the number of deposited layers per second. The substrate temperature, which is denoted by T, has a strong influence of the migration rate via the Arrhenius rate law.

Specifically, when the thin film is deposited at a low temperature/high adsorption rate, e.g., $T = 400$ K and $W = 1$ layer/s, a porous film microstructure is obtained due to the limited mobility of the particles compared to the deposition rate; while at high temperature/low adsorption rate, e.g., $T = 400$ K and $W = 1$ layer/s, the film is more likely to be dense with a flat surface, since the migration process is significant and on-film particles can move to more stable sites before new particles arrive.

2.2 Definition of variables

In this section, the variables that characterize the film surface morphology are defined. Surface height profile represents the film surface morphology and is defined as the connection of the centers of the surface particles (see Fig. 2). From a measurement point of view, surface particles are the particles that can be reached from above in the vertical direction without being fully blocked by other particles on the film (Hu et al. (2009d,a)). Surface roughness is a commonly used measure of thin film surface morphology and is defined as the root-mean-square (RMS) of surface height profile in the following form:

$$r = \left[\frac{1}{2L} \sum_{i=1}^{2L} (h_i - \bar{h})^2 \right]^{1/2}, \qquad (1)$$

where r denotes surface roughness, h_i, $i = 1, 2, \ldots, 2L$, is the surface height at the i-th position in the unit of layer, L is the number of sites in the lattice on the lateral direction, and $\bar{h} = \frac{1}{2L}\sum_{i=1}^{2L} h_i$ is the average surface height.

In addition to surface roughness, the gradient (slope) of surface height profile is another important variable that determines the surface morphology. In this work, the root-mean-square (RMS) slope represents the extent of surface slope and is defined in a similar fashion to surface roughness as follows:

$$m = \left[\frac{3}{2L} \sum_{i=1}^{2L} (h_i - h_{i+1})^2 \right]^{1/2}, \qquad (2)$$

where m denotes the RMS slope, which is a dimensionless variable, and the numerator of the fraction, 3, is the unit value of slope square and equals the square of the geometric ratio, $\sqrt{3}$, in a triangular lattice. We note that due to the PBCs, the slope at the last lattice site ($i = 2L$) is computed as the surface height difference between the last lattice site and the first lattice site. Fig. 2 shows an example of the surface slope obtained from the surface height profile.

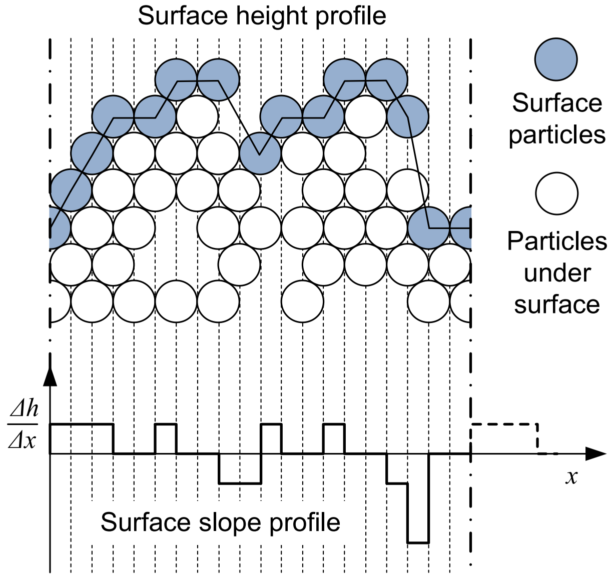

Fig. 2. An example showing the definition of the surface height profile and the calculation of the corresponding surface slope profile. It can be seen that the surface slope is always a multiple of $\sqrt{3}$, which is the geometric ratio in the triangular lattice.

The two variables which are related to the surface morphology, surface roughness and RMS slope, are defined in a similar fashion, i.e., root mean squares of a spatial profile. However, surface roughness is calculated on the basis of the surface height profile, while RMS slope is based on the surface slope profile. Thus, the two variables describe different properties of the surface height profile. Surface roughness measures the correlation of surface height at all sites, and thus, the sequence of the surface sites does not affect the calculation of surface roughness. On the contrary, surface slope is the height difference between two adjacent surface sites. As a result, RMS slope measures the height correlation of adjacent surface sites and is sensitive to the sequence of surface sites. Therefore, two surface profiles with the same roughness may have very different RMS slope profiles. We also note that surface roughness and RMS slope are not fully independent. In the extreme case of a flat surface, both surface roughness and RMS slope have zero values.

3. RMS SLOPE BEHAVIOR

In this section, the RMS slope is calculated from the surface height profile of the thin film deposition process. The behavior of RMS slope, i.e., its dynamics and dependence on lattice size, is then investigated. For the convenience of theoretical analysis and comparison with the simulations, the square of RMS slope (mean slope square), i.e., $m^2 = \frac{3}{2L}\sum_{i=1}^{2L}(h_i - h_{i+1})^2$, is used.

3.1 Dynamics of RMS slope

To investigate the dynamics of RMS slope, kMC simulations of the thin film deposition process are carried out with fixed substrate temperature and adsorption rate throughout the entire simulation. The lattice size is fixed to 100 sites in this section. The simulation duration is large enough to allow the RMS slope to reach its steady-state value. Due to the stochastic nature of kMC methods, different simulation runs may result in different lattice configurations and different surface morphology. Multiple independent simulations runs (10,000 to 25,000 runs) are carried out to generate smooth profiles of statistical moments, i.e., expected values and variances.

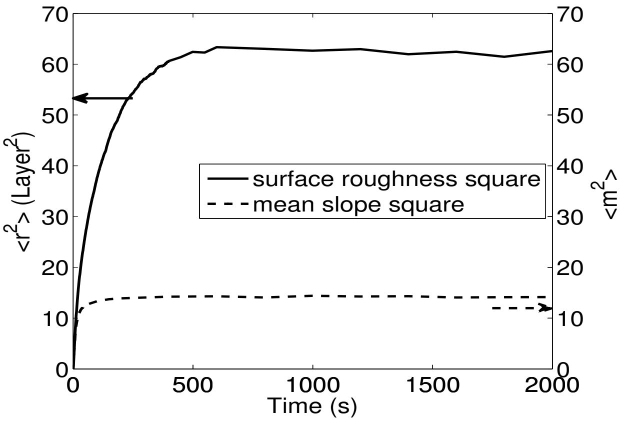

Fig. 3. Profiles of the expected mean slope square (dashed line) and surface roughness square (solid line) from kMC simulations with lattice size of $L = 100$; $W = 1$ layer/s and $T = 300$ K.

Fig. 3 shows the profile of the expected mean slope square at a substrate temperature of 300 K and an adsorption rate of 1.0 layer/s. Fig. 3 also includes the profile of the corresponding expected roughness square. The mean slope square profile evolves similarly to the roughness square profile: mean slope square increases from zero and approaches a finite steady-state value at large times. However, the dynamics of surface roughness square and mean slope square are different in many aspects. First, the mean slope square has faster dynamics than roughness square. Second, the value of the expected mean slope square is smaller than the steady-state value of roughness square (the presence of the $\sqrt{3}$ term in the RMS slope definition of (2) does not change this relationship). These differences indicate different height correlations that surface roughness and RMS slope measure. The height correlation of adjacent surface sites, which mean slope square measures, is higher than the surface height correlation with the average height which is measured by the surface roughness. The higher correlation results in a smaller difference, i.e., a smaller value and faster dynamics of mean slope square than surface roughness. KMC simulations have also been carried out at different operating conditions, e.g., different substrate temperatures or adsorption rates. A consistent trend has been observed for surface roughness and RMS slope, i.e., the two variables both increase or decrease as the operating conditions change (detailed results are omitted due to space limitations). This consistency indicates that RMS slope and surface roughness can be captured by the same analytical dynamic equation of the surface height profile, as we will discuss below.

3.2 Lattice-size dependence of RMS slope

To investigate the dependence of RMS slope on lattice size, kMC simulations of the thin film deposition process are carried out for different lattice sizes (from 20 to 500). The operating conditions are fixed at $T = 300$ K and $W = 1.0$ layer/s for all simulations. Fig. 4 shows the

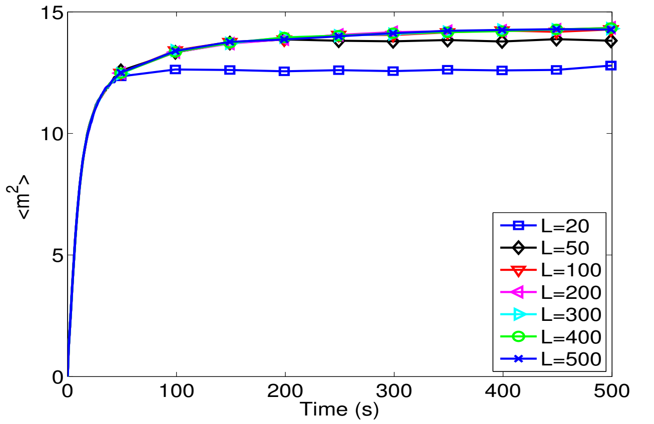

Fig. 4. Profiles of the expected mean slope square from kMC simulations with different lattice sizes; $W = 1$ layer/s and $T = 300$ K.

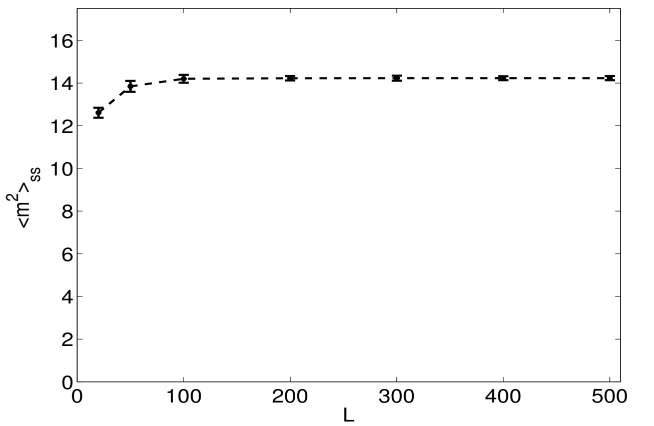

Fig. 5. Dependence of the steady-state values of the expected mean slope square with error bars, $\langle m^2 \rangle_{ss}$, from kMC simulations, on the domain size, L; $W = 1$ layer/s and $T = 300$ K.

profiles of the expected mean slope square for different lattice sizes with error bars calculated from 20 averages of evenly-divided groups of all simulation runs. From Fig. 4, it can be seen that the dynamics of mean slope square have a weak relationship with the lattice size at large lattice sizes, i.e., the profiles of mean slope square evolve and reach steady state in a short time regardless of the lattice sizes. Similar to the dynamics, the steady-state values of mean slope square also have a weak dependence on lattice size, especially at large lattice sizes. This weak dependence of steady-state values on lattice size can be addressed more clearly in Fig. 5, which plots the steady-state values versus the lattice size. In the next section, analytical and numerical results will be obtained and discussed from a stochastic PDE model of the thin film deposition process under consideration to explain the behavior of the expected mean slope square observed by the simulations.

4. ANALYTICAL AND NUMERICAL RESULTS FROM STOCHASTIC PDE MODEL

The dynamics and evolution of the surface height profile of the thin film growth process of Fig. 1 can be described by an Edwards-Wilkinson (EW)-type equation, which is a second-order stochastic PDE (Edwards and Wilkinson (1982); Family (1986); Hu et al. (2009a)).

In the EW equation, $h(x,t)$ represents the surface height profile in the continuum spatial domain case and takes the following form (Edwards and Wilkinson (1982); Hu et al. (2009a)):

$$\frac{\partial h}{\partial t} = r_h + \nu \frac{\partial^2 h}{\partial x^2} + \xi(x,t), \tag{3}$$

subject to the following periodic boundary conditions (PBCs):

$$h(-L_0,t) = h(L_0,t), \quad \frac{\partial h}{\partial x}(-L_0,t) = \frac{\partial h}{\partial x}(L_0,t) \tag{4}$$

and the initial condition:

$$h(x,0) = h_0(x), \tag{5}$$

where $x \in [-L_0, L_0]$ is the spatial coordinate, t is the time, and $\xi(x,t)$ is a Gaussian white noise with the following expressions for its mean and covariance:

$$\begin{aligned} \langle \xi(x,t) \rangle &= 0, \\ \langle \xi(x,t)\xi(x',t') \rangle &= \sigma^2 \delta(x-x')\delta(t-t'), \end{aligned} \tag{6}$$

where $\langle \cdot \rangle$ denotes the mean value, σ^2 is a parameter which measures the intensity of the Gaussian white noise and $\delta(\cdot)$ denotes the standard Dirac delta function.

In the EW equation of (3), r_h, ν, and σ^2 are model parameters. Specifically, r_h is related to the growth of the average surface height, ν is related to the effect of surface particle relaxation and migration, and σ^2 is related to the noise intensity. Since r_h is only related to the average surface height, this term can be ignored for the purposes of studying the dynamics and scaling behavior of surface roughness and RMS slope, i.e., $r_h = 0$ (Hu et al. (2009a)).

4.1 Analytical derivation

The behavior of surface roughness can be derived from the EW equation (3). For the expected surface roughness square, the steady-state value scales linearly with the domain size in a one-dimensional domain in space. This lattice-size dependence is consistent with the kMC simulation results of the thin film deposition process (Hu et al. (2009a)).

The dynamics of RMS slope can be derived from the EW equation using modal decomposition. A direct computation of the following eigenvalue problem of the linear operator of (3) subject to the PBCs of (4):

$$\begin{aligned} \nu \frac{d^2 \bar{\phi}_n(x)}{dx^2} &= \lambda_n \bar{\phi}_n(x), \\ \bar{\phi}_n(-L_0) = \bar{\phi}_n(L_0), \quad \frac{d\bar{\phi}_n}{dx}(-L_0) &= \frac{d\bar{\phi}_n}{dx}(L_0) \end{aligned} \tag{7}$$

yields the following solution for the eigenvalues, λ_n, and the eigenfunctions, $\bar{\phi}_n(x)$:

$$\begin{aligned} \lambda_n &= -\nu k^2 n^2 \\ \phi_n(x) = c_n \sin(knx), &\quad \psi_n(x) = c_n \cos(knx) \end{aligned} \tag{8}$$

where $\phi_n(x)$ and $\psi_n(x)$ are the two eigenfunctions corresponding to the same non-zero eigenvalue λ_n, $n \geq 1$, with a multiplicity of 2, $k = \frac{\pi}{L_0}$ is used to satisfy the PBCs, and

c_n is introduced for the purpose of normalization with the values $c_0 = \frac{1}{\sqrt{2L_0}}$ and $c_n = \frac{1}{\sqrt{L_0}}$, $n = 1, 2, 3, \ldots$. The solution of (3) is expanded in an infinite series in terms of the eigenfunctions of the operator of (7) as follows:

$$h(x,t) = \sum_{n=0}^{\infty} \alpha_n(t)\bar{\phi}_n(x). \tag{9}$$

Substituting the above expansion for the solution, $h(x,t)$, into (3) and taking the inner product with the adjoint eigenfunctions, the following system of infinite stochastic ordinary differential equations (ODEs) is obtained:

$$\frac{d\alpha_n}{dt} = \lambda_n \alpha_n + \xi_\alpha^n(t), \quad n = 0, 1, \ldots, \infty, \tag{10}$$

where ξ_α^n is the projection of the noise $\xi(x,t)$ in the n-th ODE. Due to the linearity of the stochastic ODE system of (10), the analytical solution of state variance can be directly solved from a direct computation. Specifically, the expressions of the steady-state value of state variance are shown as follows:

$$\left\langle \alpha_n^2 \right\rangle_{ss} = -\frac{\sigma^2}{2\lambda_n}, \quad n = 1, 2, \ldots, \infty. \tag{11}$$

Similar to the discrete lattice, the continuum form of the RMS slope is defined as follows:

$$m(t) = \left\{ \frac{1}{2L_0} \int_{-L_0}^{L_0} \left[\frac{\partial h}{\partial x}(x,t) \right]^2 dx \right\}^{1/2}. \tag{12}$$

Substituting the infinite expansion of $h(x,t)$ of (9) into (12), the expected mean slope square, $\left\langle m^2(t) \right\rangle$, can be rewritten as follows:

$$\begin{aligned} \left\langle m^2(t) \right\rangle &= \left\langle \frac{1}{2L_0} \int_{-L_0}^{L_0} \left[\frac{\partial h}{\partial x}(x,t) \right]^2 dx \right\rangle \\ &= \frac{1}{2L_0} \left\langle \int_{-L_0}^{L_0} \left[\sum_{n=0}^{\infty} \alpha_n(t) \frac{\partial \bar{\phi}_n}{\partial x}(x) \right]^2 dx \right\rangle \\ &= \frac{1}{2L_0} \left\langle \int_{-L_0}^{L_0} \left[\sum_{n=0}^{\infty} \pm \alpha_n(t) k n \bar{\phi}_n(x) \right]^2 dx \right\rangle \\ &= \frac{1}{2L_0} \left\langle \sum_{n=1}^{\infty} k^2 n^2 \alpha_n^2(t) \right\rangle = \frac{1}{2L_0} \sum_{n=1}^{\infty} k^2 n^2 \left\langle \alpha_n^2(t) \right\rangle. \end{aligned} \tag{13}$$

Eq. (13) provides a direct link between the state variance of the infinite stochastic ODEs of (10) and the expected mean slope square of the surface height profile. The steady-state value of the expected mean slope square, $\left\langle m^2 \right\rangle_{ss}$, can be obtained as $t \to \infty$. By substituting the steady-state variances of (11) and the expressions of the eigenvalues of (8), the analytical form of $\left\langle m^2 \right\rangle_{ss}$ is as follows:

$$\begin{aligned} \left\langle m^2 \right\rangle_{ss} &= \frac{1}{2L_0} \sum_{n=1}^{\infty} k^2 n^2 \left\langle \alpha_n^2 \right\rangle_{ss} \\ &= -\frac{1}{2L_0} \sum_{n=1}^{\infty} k^2 n^2 \frac{\sigma^2}{2\lambda_n} = \frac{1}{2L_0} \sum_{n=1}^{\infty} \frac{\sigma^2}{2\nu} \\ &= \frac{1}{2L_0} \frac{\sigma^2}{2\nu} + \frac{1}{2L_0} \frac{\sigma^2}{2\nu} + \frac{1}{2L_0} \frac{\sigma^2}{2\nu} + \ldots. \end{aligned} \tag{14}$$

From (14), it can be seen that each state contributes an equal finite part, $\frac{1}{2L_0}\frac{\sigma^2}{2\nu}$, to the steady-state value of the expected mean slope square, $\left\langle m^2 \right\rangle_{ss}$. Since the stochastic ODE system of (10) has an infinite number of states, the steady-state value of the expected mean slope square has an infinite value. It can be also seen that $\left\langle m^2 \right\rangle_{ss}$ has a reciprocal dependence on the domain size, L_0.

4.2 Numerical results of discretized solution

In the previous section, the analytical derivation from the EW equation in a continuum domain results in an infinite steady-state value and a reciprocal domain-size dependence of the expected mean slope square. This behavior is different from the one obtained from the kMC simulations of the lattice model, which leads to a finite steady-state value and a weak lattice-size dependence. This difference does not mean that the EW equation cannot be used to describe the evolution of the surface height profile and of the RMS slope. Instead, the same behavior of RMS slope can be obtained from the EW equation under a suitable finite-difference discretization of the continuum surface height profile.

To obtain the behavior due to the finite discretization of the EW equation, numerical simulations are carried out to compute solutions of the EW equation, i.e., surface height profile. The numerical solution of the EW equation can be obtained from a high-order approximation of the infinite ODE system of (10). Due to the decoupled nature of the ODE system, the solution of each state is a stochastic process, which is independent from the other states. Since the ODE system contains infinite number of states and results in an infinite computational time for the solution, a reduced-order system with a sufficiently large number of modes is used as an approximation of the infinite full-order system. After the solution of the surface height profile is obtained, it is sampled at discrete positions to obtain a discrete surface height profile. The sampled positions are determined from a finite-difference discretization with the same number of discretization points as the lattice size in the lattice model of the thin film deposition process. Then, the expected RMS slope and the expected mean slope square can be computed from the discrete surface height profile. We note that the surface height profile is also discretized in the growth direction to represent the discrete thin film lattice model (the step size of the discretization). Since the numerical solutions are stochastic realizations of the analytical solution, multiple independent numerical solutions are obtained to calculate the expected mean slope square.

Fig. 6 shows the profile of the expected mean slope square, which is obtained from the numerical solutions of the EW equation with $\nu = 1$ and $\sigma^2 = 1$. The domain size of the EW equation ranges from $L_0 = 0.2\pi$ to $L = 5\pi$. We note that the number of discretization points, L, changes simultaneously and proportionally with the domain size. As a result, the same step size of discretization, $\Delta x = 2L_0/L$, is preserved, which corresponds to the size of particles in the lattice model. Therefore, the number of discretization points, which is also denoted by L, ranges from $L = 20$ to $L = 500$. In Fig. 6, the expected mean slope square profiles evolve similarly to the profiles from the discrete lattice kMC model shown in Fig. 3.

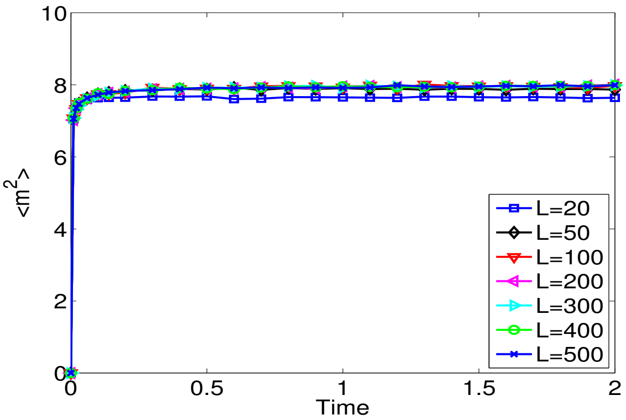

Fig. 6. Profile of the expected mean slope square from the discretized solution of the EW equation with different domain sizes; $\Delta x = 2L_0/L = 0.02\pi$.

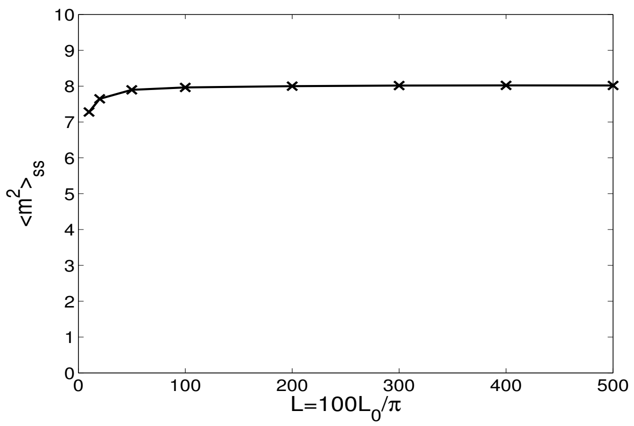

Fig. 7. Dependence of the steady-state values of the expected mean slope square, $\langle m^2 \rangle_{ss}$, from the discretized solution of the EW equation, on the domain size, L_0; $\Delta x = 2L_0/L = 0.02\pi$.

The domain-size dependence of the expected mean slope square is obtained from the numerical solutions of the EW equation with different domain sizes, L_0 ranges from 0.2π to 5π. Fig. 7 shows the domain-size dependence of the steady-state value of the expected mean slope square, which remains constant at large domain sizes.

From Figs. 6 and 7, the same behavior is observed from the discretized solution of the EW equation as the one from the kMC simulations of the lattice model, i.e., a finite steady-state value and a weak lattice-size dependence of the steady-state value of the expected mean slope square. The consistency between the discretized solution of the EW equation and of the kMC simulations corroborates the choice of the EW equation as the dynamic model for the surface height profile in the thin film deposition process under consideration. This observation of the finite steady-state value and the weak dependence on lattice size of the expected mean slope square can also be derived analytically from the EW equation on the basis of the finite discretization (see Huang et al. (2010) for detailed derivations).

REFERENCES

Christofides, P.D., Armaou, A., Lou, Y., and Varshney, A. (2008). *Control and Optimization of Multiscale Process Systems*. Birkhäuser, Boston.

Edwards, S.F. and Wilkinson, D.R. (1982). The surface statistics of a granular aggregate. *Proceedings of the Royal Society of London Series A - Mathematical Physical and Engineering Sciences*, 381, 17–31.

Family, F. (1986). Scaling of rough surfaces: effects of surface diffusion. *Journal of Physics A: Mathematical and General*, 19, L441–L446.

Hu, G., Huang, J., Orkoulas, G., and Christofides, P.D. (2009a). Investigation of film surface roughness and porosity dependence on lattice size in a porous thin film deposition process. *Physical Review E*, 80, 041122.

Hu, G., Orkoulas, G., and Christofides, P.D. (2009b). Modeling and control of film porosity in thin film deposition. *Chemical Engineering Science*, 64, 3668–3682.

Hu, G., Orkoulas, G., and Christofides, P.D. (2009c). Regulation of film thickness, surface roughness and porosity in thin film growth using deposition rate. *Chemical Engineering Science*, 64, 3903–3913.

Hu, G., Orkoulas, G., and Christofides, P.D. (2009d). Stochastic modeling and simultaneous regulation of surface roughness and porosity in thin film deposition. *Industrial & Engineering Chemistry Research*, 48, 6690–6700.

Huang, J., Hu, G., Orkoulas, G., and Christofides, P.D. (2010). Dynamics and lattice-size dependence of surface mean slope in thin film deposition. *Industrial & Engineering Chemistry Research,* submitted.

Kardar, M. (2000). Roughness and ordering of growing films. *Physica A*, 281, 295–310.

Krč, J., Smole, F., and Topič, M. (2003). Analysis of light scattering in amorphous Si:H solar cells by a one-dimensional semi-coherent optical model. *Progress in Photovoltaics: Research and Applications*, 11, 15–26.

Levine, S.W. and Clancy, P. (2000). A simple model for the growth of polycrystalline Si using the kinetic Monte Carlo simulation. *Modelling and Simulation in Materials Science and Engineering*, 8, 751–762.

Levine, S.W., Engstrom, J.R., and Clancy, P. (1998). A kinetic Monte Carlo study of the growth of Si on Si(100) at varying angles of incident deposition. *Surface Science*, 401, 112–123.

Lou, Y. and Christofides, P.D. (2003). Feedback control of growth rate and surface roughness in thin film growth. *AIChE Journal*, 49, 2099–2113.

Müller, J., Rech, B., Springer, J., and Vanecek, M. (2004). TCO and light trapping in silicon thin film solar cells. *Solar Energy*, 77, 917–930.

Ni, D. and Christofides, P.D. (2005). Multivariable predictive control of thin film deposition using a stochastic PDE model. *Industrial & Engineering Chemistry Research*, 44, 2416–2427.

Vlachos, D.G., Schmidt, L.D., and Aris, R. (1993). Kinetics of faceting of crystals in growth, etching, and equilibrium. *Physical Review B*, 47, 4896–4909.

Vorburger, T.V., Marx, E., and Lettieri, T.R. (1993). Regimes of surface roughness measurable with light scattering. *Applied Optics*, 32, 3401–3408.

Wang, L. and Clancy, P. (2001). Kinetic Monte Carlo simulation of the growth of polycrystalline Cu films. *Surface Science*, 473, 25–38.

Yang, Y.G., Johnson, R.A., and Wadley, H.N. (1997). A Monte Carlo simulation of the physical vapor deposition of nickel. *Acta Materialia*, 45, 1455–1468.

Zhang, P., Zheng, X., Wu, S., Liu, J., and He, D. (2004). Kinetic Monte Carlo simulation of Cu thin film growth. *Vacuum*, 72, 405–410.